

PHYSICS CONTRIBUTION

ELECTROMAGNETIC-GUIDED DYNAMIC MULTILEAF COLLIMATOR TRACKING ENABLES MOTION MANAGEMENT FOR INTENSITY-MODULATED ARC THERAPY

PAUL J. KEALL, PH.D.,* AMIT SAWANT, PH.D.,* BYUNGCHUL CHO, PH.D.,* DAN RUAN, PH.D.,* JUNQING WU, M.S.,* PER POULSEN, PH.D.,* JAY PETERSEN, M.S.,† LAURENCE J. NEWELL, M.S.,† HERBERT CATTELL, B.A.,‡ AND STINE KORREMAN, PH.D.§||

*Department of Radiation Oncology, Stanford University, Stanford, CA; †Calypso Medical Technologies, Seattle, WA; ‡Varian Medical Systems, Palo Alto, CA; §Rigshospitalet, University of Copenhagen, Copenhagen, Denmark, and ||Department of Human Oncology, University of Wisconsin-Madison, Madison, WI

Purpose: Intensity-modulated arc therapy (IMAT) is attractive because of high-dose conformality and efficient delivery. However, managing intrafraction motion is challenging for IMAT. The purpose of this research was to develop and investigate electromagnetically guided dynamic multileaf collimator (DMLC) tracking as an enabling technology to treat moving targets during IMAT.

Methods and Materials: A real-time three-dimensional DMLC-based target tracking system was developed and integrated with a linear accelerator. The DMLC tracking software inputs a real-time electromagnetically measured target position and the IMAT plan, and dynamically creates new leaf positions directed at the moving target. Low- and high-modulation IMAT plans were created for lung and prostate cancer cases. The IMAT plans were delivered to a three-axis motion platform programmed with measured patient motion. Dosimetric measurements were acquired by placing an ion chamber array on the moving platform. Measurements were acquired with tracking, without tracking (current clinical practice), and with the phantom in a static position (reference). Analysis of dose distribution differences from the static reference used a γ -test.

Results: On average, 1.6% of dose points for the lung plans and 1.2% of points for the prostate plans failed the 3-mm/3% γ -test with tracking; without tracking, 34% and 14% (respectively) of points failed the γ -test. The delivery time was the same with and without tracking.

Conclusions: Electromagnetic-guided DMLC target tracking with IMAT has been investigated for the first time. Dose distributions to moving targets with DMLC tracking were significantly superior to those without tracking. There was no loss of treatment efficiency with DMLC tracking. © 2011 Elsevier Inc.

Motion management, tumor tracking, arc therapy.

INTRODUCTION

The purpose of this research was to develop and investigate electromagnetic-guided dynamic multileaf collimator (DMLC) tracking as an enabling technology to treat moving targets during intensity-modulated arc therapy (IMAT).

IMAT is attractive because of high-dose conformality and efficient delivery (1–3). However, managing intrafraction motion is challenging for rotational therapy techniques. Gating is not suitable, as a heavy rotating gantry needs to be quickly and repeatedly started and stopped, and gated

Reprint requests to: Paul Keall, Ph.D., Radiation Physics Division, Department of Radiation Oncology, Stanford University, 875 Blake Wilbur Drive, Room G-210, Stanford, CA 94305-5847. Tel: (650) 723-5549; Fax: (650) 498-5008; E-mail: paul.keall@stanford.edu

Supported by Calypso Medical Technologies, Varian, and the National Institutes of Health (R01 93626).

Conflict of interest: J.P. and L.J.N. are employed by Calypso Medical Technologies, and H.C. is employed by Varian Medical Systems.

Acknowledgments—The authors appreciate the use of the lung motion data provided by Sonja Dieterich (Stanford), the prostate motion data provided by Patrick Kupelian and Katja Langen (MD Anderson Orlando), rotation matrix coding by David Carlson (now at Yale), Rapidarc planning from Ed Mok (Stanford), phantom modifications from Fred van den Haak (Stanford), and experimental

assistance from Yolanda Aarons (Peter MacCallum Institute), Marianne Falk (Rigshospitalet, Copenhagen, and Lund University), and Yelin Suh (Stanford). Mark Wanlass (Stanford) answered many machine-related pages in the late evening and on weekends. The authors thank Michelle Svatos (Varian), who contributed to and supported this project in many aspects and was instrumental in bringing the hardware components together. Thanks are also expressed to Libby Roberts (Stanford) for reviewing the manuscript and improving the clarity. Research support from Calypso Medical Technologies, Varian Medical Systems, and the National Institutes of Health is gratefully acknowledged. Thanks also are expressed to the reviewers whose observations and suggestions substantially improved the clarity of the manuscript.

Received Oct 16, 2009, and in revised form Feb 27, 2010. Accepted for publication March 4, 2010.

delivery is inefficient. An attractive solution that reduces the mechanical stress and increases efficiency is to use the dynamic multileaf collimator (DMLC) to track the moving target when real-time target motion data are available. Other potential motion management solutions for IMAT (not discussed here) are couch tracking, breath hold, and abdominal compression techniques.

DMLC tracking has been experimentally investigated on Accuknife (1), Siemens (2), Tomotherapy (3), and Varian (4–11) systems. Based on publication dates, the number of research groups and companies interested in DMLC tracking is growing rapidly, although, to our knowledge, DMLC tracking has yet to be implemented for patient treatments.

A method to monitor real-time target motion during radiotherapy delivery is the Calypso 4D Localization system (Calypso Medical Technologies, Seattle, WA), which uses electromagnetic radiation to localize implanted transponders with respect to a planar array, and optical tracking to determine the array position. Balter *et al.* (12) demonstrated sub-millimeter system accuracy for static and dynamic motion up to $3 \text{ cm} \cdot \text{s}^{-1}$. Sawant *et al.* (13), using an earlier version of the integrated DMLC tracking system used for the current experiments, showed the system geometric accuracy to be less than 2 mm for lung and 1 mm for prostate motion. With the same system used for the Sawant geometric accuracy measurements, Smith *et al.* (14) quantified the dosimetric accuracy and found that tracking dose measurements were similar to the gating measurements for intensity-modulated radiation therapy (IMRT), with a 2–5 fold increase in delivery efficiency for tracking compared with gating.

In this study, we describe the implementation and dosimetric investigation of electromagnetic-guided DMLC tracking during IMAT using clinically realistic plans and patient-derived motion traces.

METHODS AND MATERIALS

The clinical focus of this study concentrated on lung and prostate cancer. Lung tumors were chosen because of the motion magnitude and complexity, and the canine (15) and human (16) lung investigations with the Calypso system. Prostate cancer was chosen because significant complex motion is seen in some (17) cases, and the Calypso system has been cleared by the Food and Drug Administration for clinical radiotherapy treatments in the prostate.

Motion traces and IMAT plans

The goal of this study was to span the complexity of motion and IMAT modulation that may be expected in clinical practice. Although it is clearly difficult, if not impossible, to span the entire spectrum of clinical variability, to achieve varied motion, motion files of higher than average motion magnitudes and complexity were selected from large abdominal/thoracic (18) and prostate (17) motion databases. The selected abdominal/thoracic traces were all from lung tumors as used by Poulsen *et al.* (9) representing “typical” motion, high-frequency breathing, predominantly left-right motion, and baseline variations. The selected prostate cases represent continuous drift, persistent excursion, transient excursion,

and high frequency excursions as used by Poulsen *et al.* (10). The motion files used for the current study are shown in Fig. 1. Consistent with the Poulsen studies, and to allow the prediction algorithm 20 s of learning time, the beam was started 20 s after the start of the data files (pre-beam-on data are not shown in Fig. 1, but the phantom center was at the isocenter (0,0,0) 20 s before the beam initiation). The phantom motion and treatment initiation were approximately the same for the tracking and without tracking measurements.

The IMAT plans were created using the RapidArc software in the Eclipse Treatment Planning System (version 8.6) from Varian. To include different patient motions, lung (larger motion with a periodic motion component) and prostate (smaller motion with a random motion component) plans were created based on patients treated with RapidArc at Stanford. Plans with low modulation (by optimizing only the PTV dose), and high modulation (by optimizing the PTV and critical structures with difficult constraints) were created to span the range of clinical complexity. The lung plan monitor units (MUs) were 342 and 596 for the low- and high-modulation cases respectively, and the prostate plan MUs were 432 and 737. All arcs spanned 358° starting at 1° from the right posterior direction of a supine patient. The collimator was set to 90° to have the population-averaged major axis of respiratory motion (superior–inferior direction) (18) aligned with the MLC leaf travel direction. For all plans, 2 Gy was given to 95% of the PTV. The energy and dose rate for all plans was 6 MV and 600 MU/min, respectively, with treatments lasting approximately 1 min.

Electromagnetic-guided DMLC tracking system

The experimental set-up for the measurements is shown in Fig. 2. A real-time 3D DMLC-based target tracking system was developed and integrated with a 21EX linear accelerator (Varian Medical Systems, Palo Alto, CA). The real-time three-dimensional (3D) position input was provided by a Calypso 4D Localization system monitoring the position of embedded transponders and sent to the DMLC tracking system. For the lung motion traces, a kernel density estimation algorithm (19) was used to account for the 150-ms system latency. No prediction algorithm was used for the prostate cases. The DMLC tracking software integrated the real-time position data stream with the planned IMAT leaf sequence to dynamically create new leaf positions directed at the moving target. The modified leaf sequence accounting for the target translation was sent to the DMLC controller that actuated the leaf motion. Dosimetric measurements were acquired by placing a Seven29 2D ion chamber array (PTW, Freiburg, Germany) with 2 cm of solid water build-up material on the moving platform. The PTW has 729 vented, plane-parallel, $5 \times 5 \text{ mm}^2$ ion chambers in a 27×27 array with a center-to-center spacing of 10 mm. The Seven29 array has a small angular dependence. However, for the current study, in which the difference between delivery with and without tracking was studied, the angular variation is common to all of the delivery types and therefore is expected to have a minimal impact on the findings. An electromagnetic shielding “Faraday cage” (two layers of aluminum foil) was placed around the detector and cable to reduce the current induced in the ion chamber array by the Calypso system. Without this magnetic shielding, a dark field measurement over 1 min yielded approximately 0.2 Gy. With the magnetic shielding the dark field readings were reduced to 0.002 Gy/min and less.

For each plan and motion trace combination three delivery scenarios were considered: (1) tracking, in which electromagnetic (EM) guidance was used with DMLC tracking to deliver IMAT to the moving target representing the investigational arm of the study,

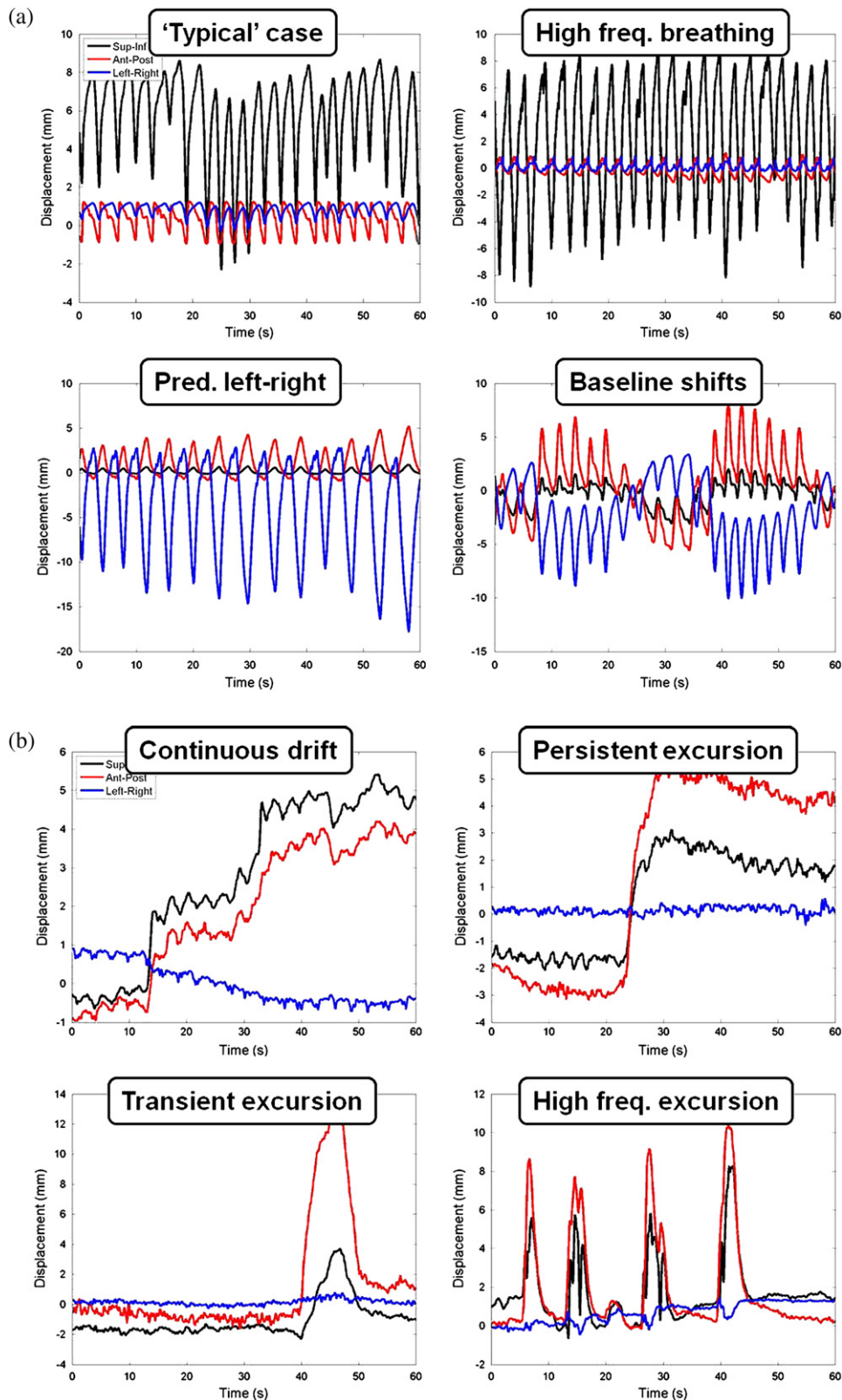


Fig. 1. (a) Lung and (b) prostate tumor motion traces used for this study, representing higher than average motion magnitude and complexity for both sites. Lung tumor sites were right hilum (typical case), right lower lobe (high frequency), right lower lobe (predominantly left-right), and left upper lobe (baseline shifts).

(2) no tracking, in which the target was moving but no modification to the planned delivery was made representing the current clinical practice of IMAT treatments, and (3) static delivery, in which the

target was not moving, used as the reference for the dynamic studies, and represents the plan that the treatment planning team evaluates on the patient anatomy.

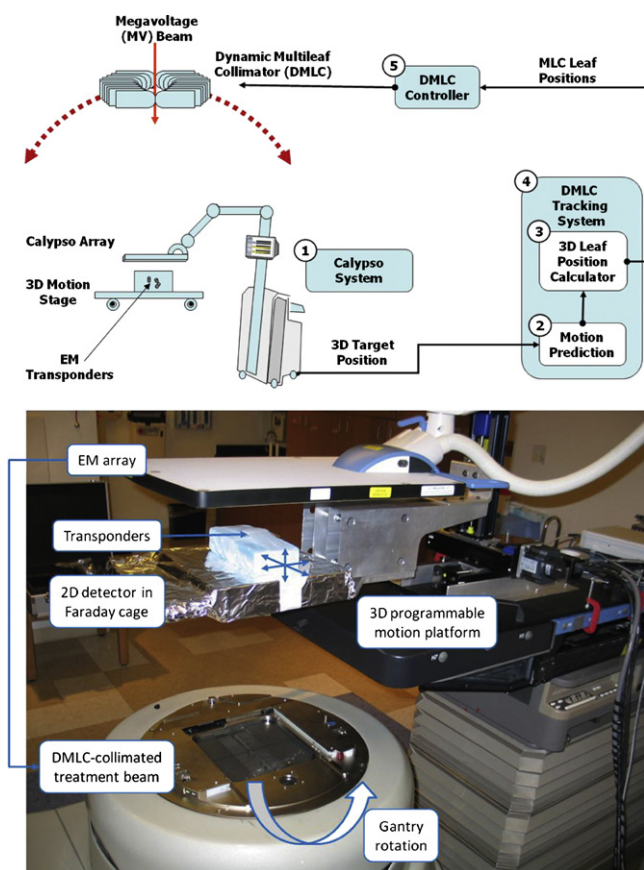


Fig. 2. Schematic diagram (top) and photograph (bottom) of the experimental set-up used for the electromagnetic-guided dynamic multileaf collimator (DMLC) tracking intensity-modulated arc therapy (IMAT) experiments.

The tracking and no-tracking dose distributions were compared with the static delivery dose using 2-mm/2% and 3-mm/3% dose difference γ -tests (20), with a 5% low-dose threshold below which comparisons were ignored. The percentage dose difference was computed relative to the maximum dose in the reference static plan. The 3-mm/3% threshold results are focused on here, as the values are commonly used clinically for IMRT QA (21), and also 3 mm corresponds to a little more than half the inner leaf width of the Millennium MLC (2.5 mm) below which, on an individual leaf basis, explicit motion compensation cannot be performed unless the leaves can be moved laterally and/or couch compensation is used. The fraction of points failing the γ -test was recorded for each plan and each tumor motion trace. The comparison method is shown in Fig. 3.

Note that the delivery of the treatment plans did not modulate the dose rate or gantry speed during the delivery, as this capability (RapidArc for the Varian linear accelerators) was not available on the accelerator used for these experiments. This limitation is unlikely to significantly affect the results or conclusions as the dose rate does variation in RapidArc does not affect the leaf position, and any modulation of the gantry speed would slow the delivery and place less stress on the leaf motion. DMLC tracking results for RapidArc delivery including dose rate or gantry speed modulation with DMLC tracking (for sinusoidal motion monitored by an optical input) have been shown by Zimmerman *et al.* (11).

All measurements were performed three times to quantify the reproducibility of the results. Statistical tests to quantify the signif-

icance of the motion tracking vs. no motion tracking γ -test results used a one-sided paired Student's *t* test.

RESULTS

Example isodose curves of comparing motion tracking and not motion tracking to the static delivery are shown in Fig. 4. The plans delivered without motion tracking tended to have misshaped and shifted dose distributions compared with the static distributions, as the short-term intrafraction motion and longer-term baseline drifts were not accounted for.

The 2-mm/2% and 3-mm/3% γ -test results over all measurements are shown in Fig. 5 and Table 1 and in Fig. 6 and Table 2, respectively. In all cases, individually and collectively, the motion tracking results showed significantly fewer points failing the γ -test than the without-motion tracking results. The three exceptions to statistical significance differences were for the 3-mm/3% γ -test low- and high-modulation lung plans for the baseline shifts traces ($p = 0.15$ and 0.07 , respectively) and low-modulation prostate plans for the transient excursion traces ($p = 0.15$). For two of these cases, the tracking results showed zero failure, and the without-tracking failures were not significantly different from zero. In some cases, the without-motion tracking results showed up to 74% 3-mm/3% γ -test failure results (low-modulation lung plan, typical tumor trace). The maximum discrepancy observed for the 3-mm/3% γ -test with motion tracking was 8% (high-modulation lung plan, baseline shift tumor trace).

For the lung plans combined (Table 2), 1.6% of the dose points failed the 3-mm/3% γ -test with tracking compared with 34% without tracking ($p < 0.001$). For the prostate plans, 1.2% and 14% of the dose points failed for the tracking and without-tracking cases, respectively ($p < 0.001$). Overall, comparing tracking to without-tracking, a 95% 3-mm/3% γ -test improvement was observed for the lung plans and 93% for the prostate plans.

IMAT plans with DMLC tracking were delivered without beam holds and completed in the same time as the delivery of the static and no-tracking plans.

DISCUSSION

EM-guided DMLC target tracking with IMAT has been investigated. Dose distributions to moving targets with DMLC tracking were significantly superior to those without tracking, although in some cases discrepancies from static delivery were observed with motion tracking. The tracking results can be further improved by faster and/or thinner leaves, lower latency, improved prediction, and planning changes. There was no loss of treatment efficiency with DMLC tracking.

The only previous publication describing dosimetric results from electromagnetic-guided DMLC tracking studied dynamic and step-and-shoot IMRT delivery but did not include arc therapy (14). Since the experiments for the previous study, significant improvements have been made to the DMLC tracking system, including general correction of “bugs” and software improvements, a different motion

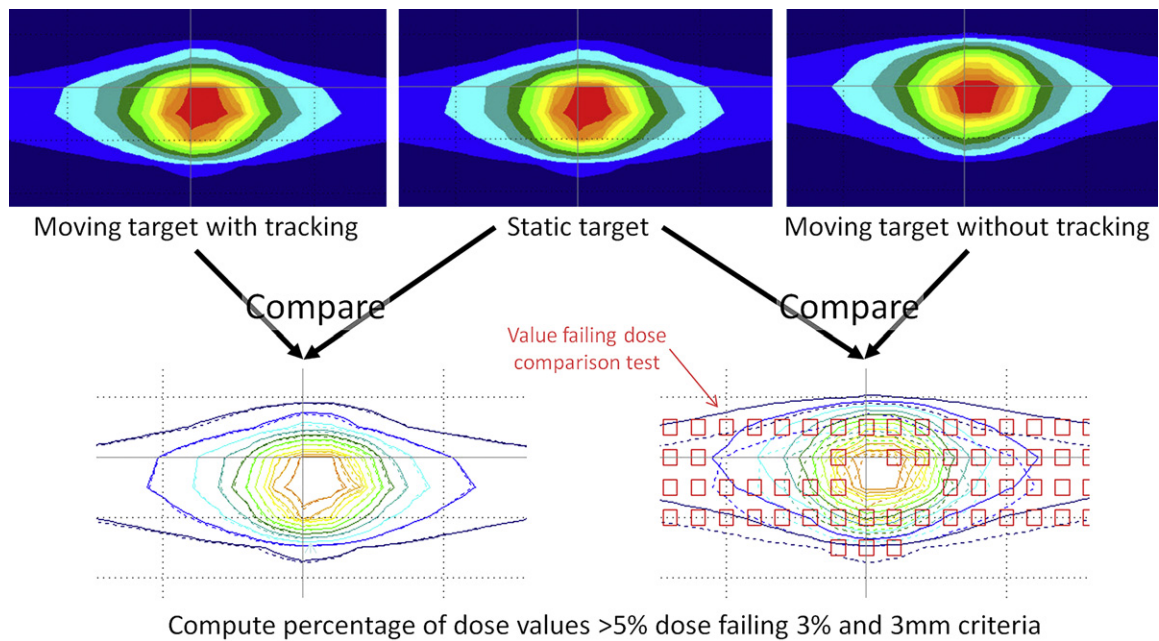


Fig. 3. Comparison method for this study. Isodose curves obtained from the moving target with and without tracking scenarios were compared with the isodose curves from delivery to a static target. Percentage of values greater than 5% of the maximum dose that failed the 3% dose difference and 3-mm distance to agreement γ criteria were computed.

prediction algorithm, with a kernel density estimation (19) rather than a modified linear adaptive filter, and a reduction in the system latency from 220 ms (13) to 150 ms (22) because of engineering improvements and hardware changes performed by Calypso. Another important change is that the number virtual sub-leaves, a parameter in the leaf sequencing code (5) was set to 1 (*i.e.*, equal to one leaf). We have found that a sub-leaf parameter value greater than 1 can be limiting for apertures in adjacent leaves spaced widely from each other that can occur in IMRT and IMAT fields, potentially placing dose in between these apertures. Improvements to the limitations of the current leaf sequencing process are currently under development (23). As expected, the benefit of motion tracking is highest when the motion is largest. Without tracking, more points failed the γ -test for the lung than the prostate; however improvements with tracking were seen for all of the plans and motion traces. There was a tendency for the tracking results to be worse as the degree of modulation increased: no points failed the γ -test with tracking for any of the motion traces for the low-modulation lung and prostate plans indicating a clear plan modulation dependence. The higher failures also appeared to occur for traces where the motion perpendicular to the leaf motion direction was significant. The left–right and anterior–posterior components of motion in Fig. 1 will be perpendicular to the leaf motion direction for gantry angles near 0/180 and 90/270, respectively, as seen for the baseline shifts (lung) and persistent excursion (prostate) traces. This limitation of accounting for target motion perpendicular to the leaf travel direction when apertures formed by adjacent leaf pairs are far apart, as can occur for IMRT and IMAT plans, is known; Fig. 1 in George *et al.* (24) is a schematic diagram of this feature. Also, motion along the leaf direction can be

corrected for continuously; the finite leaf thickness limits the resolution with which motion parallel to the leaf direction can be corrected. To alleviate this problem, during planning, in principle, the placement of these apertures could be adjusted to avoid this problem. However this would increase the constraints on the treatment plan and would degrade the plan quality as calculated by the treatment planning system, although neither the implementation nor the magnitude of this degradation at planning (and subsequent improvement in plan delivery) has been studied here. There were some

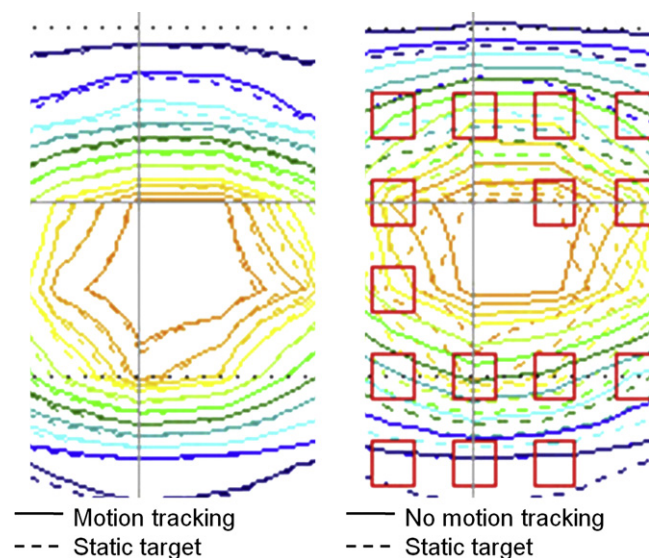


Fig. 4. Example isodose curves focused on the high-dose region. Measurements were from the low-modulation lung plan with the “typical” case motion pattern. Red squares indicate points failing the γ -test. For scale purposes, centers of adjacent red squares are 0.5 cm apart.

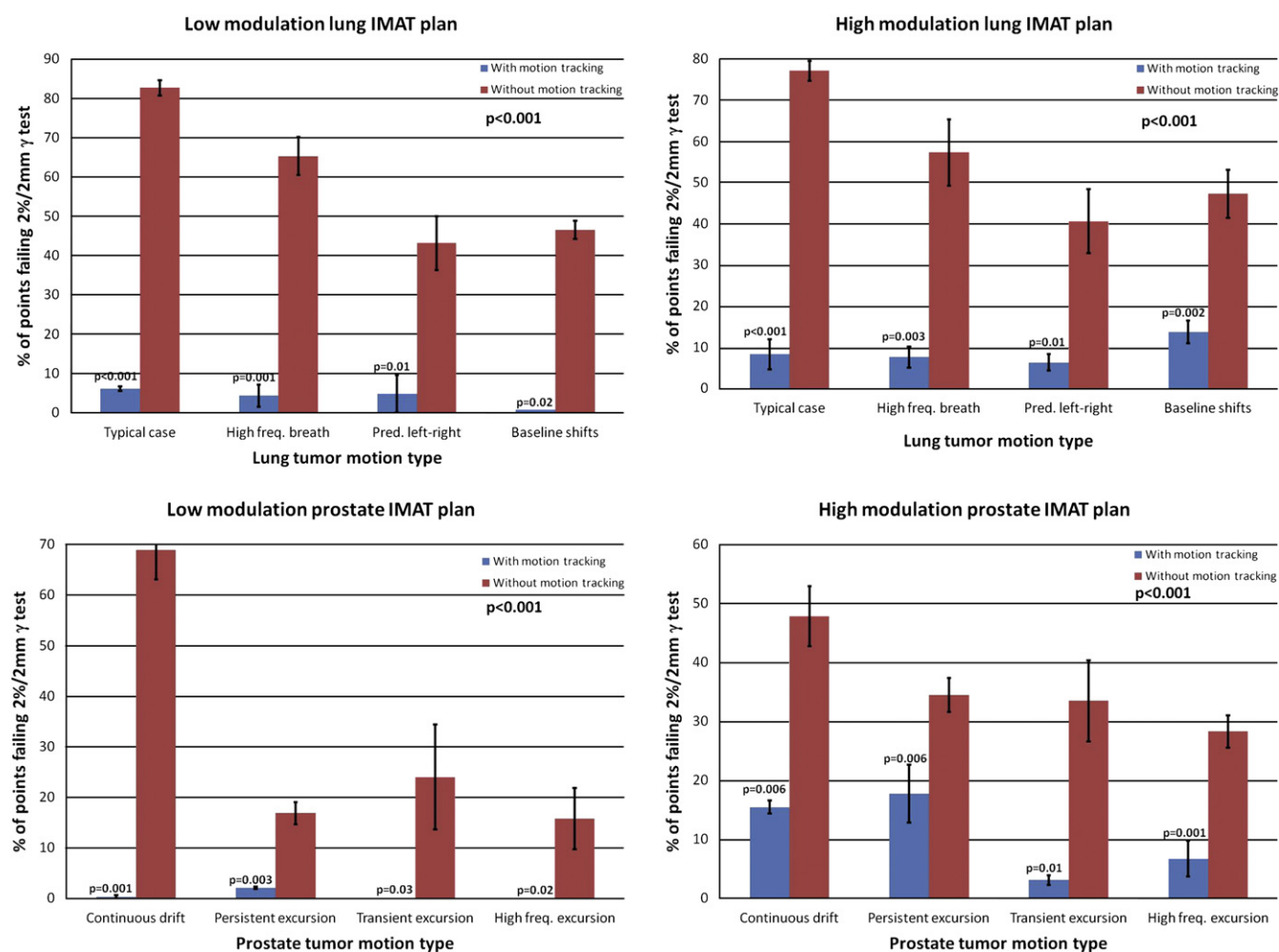


Fig. 5. Percentage of dose values that failed the 2% dose difference and 2-mm distance to agreement γ -test, with and without tracking, for the intensity-modulated arc therapy (IMAT) plan types and motion traces studied. p Values comparing with-motion tracking to without-motion tracking are given for each motion trace and also for the plan type combining all of the motion traces. Error bars are ± 1 standard deviation. Note that the y-scale is different for all four plots.

high frequency components in the traces used in this study, particularly for the prostate cases as shown in Fig. 1. These high-frequency components may be caused by measurement noise rather than by actual tumor motion, and will have the effect of increasing the requested MLC leaf motion. Having a smoother input may further reduce some of the difference between the tracking and static measurements. In addition, gating the beam when the leaves are outside tolerance would be expected to further improve the motion tracking results at the expense of increased treatment time. The current DMLC IMAT tracking approach can be considered the maximum efficiency solution, and increased accuracy could be traded off by increased treatment time and potentially gantry mechanical stress when gating arc delivery. Another method that may improve the dosimetric results for DMLC tracking is to align the collimator with the patient-observed major axis of motion. As seen in Fig. 1, tumor motion and direction change from patient to patient and with time. Also, for arc radiotherapy, the angle of the major axis of tumor motion will change as the gantry rotates for all motion apart from pure superior-inferior motion.

The difference in the dose distributions without motion tracking is caused by a combination of the shift in the target position from the initial set-up point before treatment, and shifts in the baseline position and motion during treatment causing the “interplay” effect initially described by Yu *et al.* (25) with further theoretical (26–29) and experimental (30–33) studies by several groups. The estimated dosimetric

Table 1. Summary of the average number of values failing the 2% dose difference 2-mm distance to agreement γ -test for all experiments

| Plan type and motion trace | With tracking | Without tracking | % Reduction | p Value |
|----------------------------|---------------|------------------|-------------|-----------|
| Low modulation lung | 4.1% | 59% | 93% | <0.001 |
| High modulation lung | 9.1% | 56% | 84% | <0.001 |
| Combined lung | 6.6% | 58% | 89% | <0.001 |
| Low modulation prostate | 0.6% | 31% | 98% | <0.001 |
| High modulation prostate | 11% | 36% | 70% | <0.001 |
| Combined prostate | 5.7% | 34% | 83% | <0.001 |
| All combined | 6.1% | 46% | 86% | <0.001 |

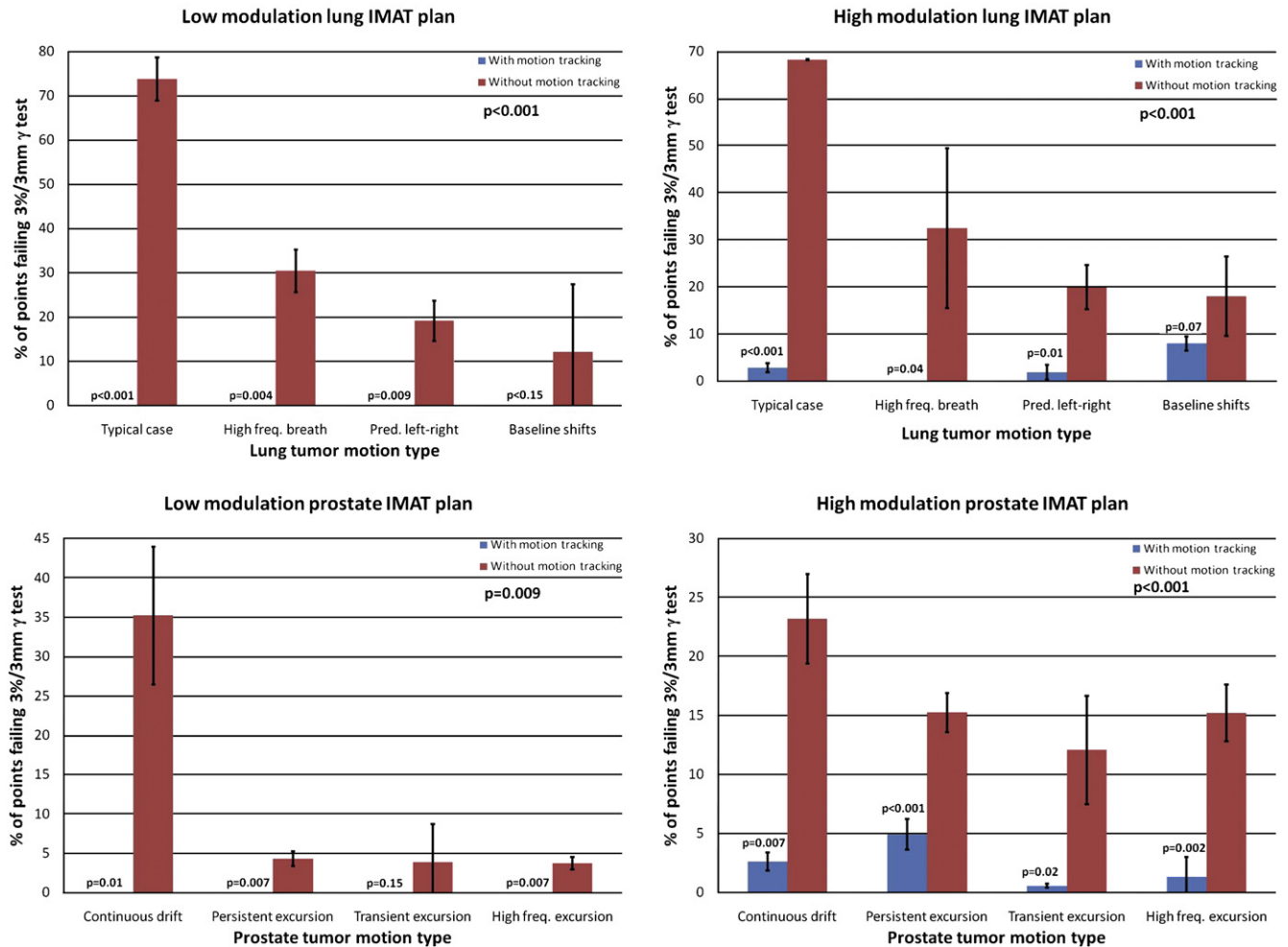


Fig. 6. Percentage of dose values that failed the 3% dose difference and 3-mm distance to agreement γ -test with and without tracking for the intensity-modulated arc therapy (IMAT) plan types and motion traces studied. *p* Values comparing with-motion tracking to without-motion tracking are given for each motion trace and also for the plan type combining all of the motion traces. Error bars are ± 1 standard deviation. Note that the y-scale is different for all four plots and different from that in Fig. 5.

impact of the interplay effect varies widely between these studies and is a combination of the target motion pattern, delivery complexity, and delivery time. In the current study the worst result from a dosimetric perspective was without motion tracking for the lung “typical case” trace and low-modulation plan. This trace exhibits a shift between the initial set-up point (the target was at the isocenter 20 s before starting beam delivery in this study) as well as large motion during the treatment. The dosimetric effects are shown in Fig. 4, where the without tracking results are shifted and misshaped with respect to the static distribution. If the target position had been monitored during treatment, the shift could have been corrected for. The results for the other three lung traces (high-frequency breathing, predominantly left–right motion, and baseline shifts) do not exhibit this shift before treatment, and the results are more indicative of the interplay effect only rather than the combined shift and interplay effect.

An important observation from the repeat measurements (Figs. 5 and 6) is the large variability in the dosimetric

results without motion tracking. For these experiments, both with and without tracking, the phantom motion and beam delivery were started at approximately the same time (variability of seconds). This large-dose variability without tracking for repeat experiments, even for the same motion

Table 2. Summary of average number of values failing the 3% dose difference 3-mm distance to agreement γ -test for all experiments

| Plan type and motion trace | With tracking | Without tracking | % Reduction | <i>p</i> Value |
|----------------------------|---------------|------------------|-------------|----------------|
| Low modulation lung | 0% | 34% | 100% | <0.001 |
| High modulation lung | 3.2% | 35% | 91% | <0.001 |
| Combined lung | 1.6% | 34% | 95% | <0.001 |
| Low modulation prostate | 0% | 12% | 100% | 0.009 |
| High modulation prostate | 2.4% | 16% | 85% | <0.001 |
| Combined prostate | 1.2% | 14% | 93% | <0.001 |
| All combined | 1.4% | 24% | 94% | <0.001 |

trace, implies that the measurement results—and hence the absorbed dose to patients—are not predictable and are sensitive to the motion magnitude and pattern, which will change with time for each patient.

The lung and prostate motion traces here had higher than “normal” patient motion; however they were patient derived, and therefore the measured results can be applied to estimate the difference in dose delivered to the patient compared with that from the plan for certain clinical situations. The prostate motion was considerably less than that of the lung, but in most of the prostate cases studied, more than 5% of the points failed the γ -test without tracking. The dosimetric results without tracking for many of these cases would not pass normal pretreatment QA guidelines. The American Association of Physicists in Medicine (AAPM) Task Group 119 Report (21) showed that, for an IMRT prostate dosimetry study comparing planned and delivered doses to static targets, on average, 2% of points failed the 3-mm/3% γ -test. Comparing tracking with static target results showed, on average, less than 2% (1.2%) 3-mm/3% γ -test disagreement. The without-tracking to static delivery results showed, on average, 14% γ -test disagreement, seven times the disagreement of that found during the AAPM Task Group 119 study. This result indicates that unaccounted-for motion may be a significantly larger source of error in treatment delivery than all of the contributing factors between planned and delivered doses to static targets combined.

The current study was performed on research systems that are not cleared by the Food and Drug Administration for clinical use; however the dosimetric results on the phantom cases are compelling, and clinical implementation will allow more accurate radiotherapy for improved patient care.

A limitation of the current study is that only target translation was accounted for; further work, should such information be available, could include accounting for real-time tumor rotation and/or deformation. Rotation of more than 30° for prostate tumors (34) and more than 45° for lung tumors (35) have been observed, indicating an important future direction for real-time tumor tracking.

CONCLUSION

For the first time, electromagnetic-guided DMLC target tracking with IMAT has been demonstrated to account for lung and prostate motion during treatment delivery. Dose distributions to moving targets with DMLC tracking were significantly superior to those without tracking. On average, 1.6% of points for the lung plans and 1.2% points for the prostate plans failed the 3-mm/3% γ -test with tracking; without tracking, 34% and 14% of points, respectively, failed the γ -test. There was no loss of treatment efficiency with DMLC tracking. This promising method uses research software integrated with commercially available position monitoring (Calypso) and delivery (Varian) hardware, and therefore has a clear path to clinical implementation.

REFERENCES

- Liu Y, Shi C, Lin B, *et al.* Delivery of four-dimensional radiotherapy with TrackBeam for moving target using an AccuKnife dual-layer MLC: Dynamic phantoms study. *J Appl Clin Med Phys* 2009;10:21–33.
- Tacke M, Nill S, Oelfke U. Real-time tracking of tumor motions and deformations along the leaf travel direction with the aid of a synchronized dynamic MLC leaf sequencer. *Phys Med Biol* 2007;52:N505–N512.
- Lu W, Mauer C, Chen M, *et al.* Experimental validation for real-time motion adapted optimization (MAO) guided delivery [abstract]. *Int J Radiat Oncol Biol Phys* 2008;72:S26.
- Keall PJ, Cattell H, Pokhrel D, *et al.* Geometric accuracy of a real-time target tracking system with dynamic multileaf collimator tracking system. *Int J Radiat Oncol Biol Phys* 2006;65:1579–1584.
- Sawant A, Venkat R, Srivastava V, *et al.* Management of three-dimensional intrafraction motion through real-time DMLC tracking. *Med Phys* 2008;35:2050–2061.
- Han-Oh S, Yi BY, Berman BL, *et al.* Usefulness of guided breathing for dose rate-regulated tracking. *Int J Radiat Oncol Biol Phys* 2009;73:594–600.
- Yi BY, Han-Oh S, Lerma F, *et al.* Real-time tumor tracking with preprogrammed dynamic multileaf-collimator motion and adaptive dose-rate regulation. *Med Phys* 2008;35:3955–3962.
- Cho B, Poulsen PR, Sloutsky A, *et al.* First demonstration of combined kV/MV image-guided real-time dynamic multileaf-collimator target tracking. *Int J Radiat Oncol Biol Phys* 2009;74:859–867.
- Poulsen PR, Cho BC, Ruan D, *et al.* Dynamic MLC tracking of respiratory target motion based on a single kilovoltage imager during arc radiotherapy. *Int J Radiat Oncol Biol Phys* (in press).
- Poulsen PR, Cho B, Sawant A, *et al.* Implementation of a new method for dynamic multileaf collimator tracking of prostate motion in arc radiotherapy using a single kV imager. *Int J Radiat Oncol Biol Phys* 2010;76:914–923.
- Zimmerman J, Korreman S, Persson G, *et al.* DMLC motion tracking of moving targets for intensity modulated arc therapy treatment: A feasibility study. *Acta Oncol* 2009;48:245–250.
- Balter JM, Wright JN, Newell LJ, *et al.* Accuracy of a wireless localization system for radiotherapy. *Int J Radiat Oncol Biol Phys* 2005;61:933–937.
- Sawant A, Smith RL, Venkat RB, *et al.* Toward submillimeter accuracy in the management of intrafraction motion: The integration of real-time internal position monitoring and multileaf collimator target tracking. *Int J Radiat Oncol Biol Phys* 2009;74:575–582.
- Smith RL, Sawant A, Santanam L, *et al.* Integration of real-time internal electromagnetic position monitoring coupled with dynamic multileaf collimator tracking: An intensity-modulated radiation therapy feasibility study. *Int J Radiat Oncol Biol Phys* 2009;74:868–875.
- Mayse ML, Parikh PJ, Lechleiter KM, *et al.* Bronchoscopic implantation of a novel wireless electromagnetic transponder in the canine lung: A feasibility study. *Int J Radiat Oncol Biol Phys* 2008;72:93–98.
- Willoughby TR, Shah AP, Forbes AR, *et al.* Clinical use of electromagnetic guidance for lung and spine radiation therapy. *Int J Radiat Oncol Biol Phys* 2008;72:S642–S643.
- Langen KM, Willoughby TR, Meeks SL, *et al.* Observations on real-time prostate gland motion using electromagnetic tracking. *Int J Radiat Oncol Biol Phys* 2008;71:1084–1090.
- Suh Y, Dieterich S, Cho B, *et al.* An analysis of thoracic and abdominal tumour motion for stereotactic body radiotherapy patients. *Phys Med Biol* 2008;53:3623–3640.

19. Ruan D. Kernel density estimation-based real-time prediction for respiratory motion. *Phys Med Biol* 2010;55:1311–1326.
20. Low DA, Harms WB, Mutic S, *et al.* A technique for the quantitative evaluation of dose distributions. *Med Phys* 1998;25:656–661.
21. Ezzell GA, Burmeister JW, Dogan N, *et al.* IMRT commissioning: Multiple institution planning and dosimetry comparisons, a report from AAPM Task Group 119. *Med Phys* 2009;36:5359–5373.
22. Sawant A, Cho B, Poulsen P, *et al.* Performance analysis of an electromagnetic transponder-based DMLC tracking system for 4D radiotherapy delivery [abstract]. *Int J Radiat Oncol Biol Phys* 2009;75:S575–S576.
23. Ruan D, Poulsen P, Cho B, *et al.* A novel optimization based leaf sequencing algorithm with explicit underdose and overdose penalties in 4D radiotherapy. *Int J Radiat Oncol Biol Phys* 2009;75:S627.
24. George R, Suh Y, Murphy M, *et al.* On the accuracy of a moving average algorithm for target tracking during radiation therapy treatment delivery. *Med Phys* 2008;35:2356–2365.
25. Yu CX, Jaffray DA, Wong JW. The effects of intra-fraction organ motion on the delivery of dynamic intensity modulation. *Phys Med Biol* 1998;43:91–104.
26. Bortfeld T, Jiang SB, Rietzel E. Effects of motion on the total dose distribution. *Semin Radiat Oncol* 2004;14:41–51.
27. Bortfeld T, Jokivarsi K, Goitein M, *et al.* Effects of intra-fraction motion on IMRT dose delivery: Statistical analysis and simulation. *Phys Med Biol* 2002;47:2203–2220.
28. Kissick MW, Boswell SA, Jeraj R, *et al.* Confirmation, refinement, and extension of a study in intrafraction motion interplay with sliding jaw motion. *Med Phys* 2005;32:2346–2350.
29. Kissick MW, Flynn RT, Westerly DC, *et al.* On the impact of longitudinal breathing motion randomness for tomotherapy delivery. *Phys Med Biol* 2008;53:4855–4873.
30. Keall PJ, Kini VR, Vedam SS, *et al.* Motion adaptive x-ray therapy: A feasibility study. *Phys Med Biol* 2001;46:1–10.
31. Jiang SB, Pope C, Al Jarrah KM, *et al.* An experimental investigation on intra-fractional organ motion effects in lung IMRT treatments. *Phys Med Biol* 2003;48:1773–1784.
32. Schaefer M, Munter MW, Thilmann C, *et al.* Influence of intra-fractional breathing movement in step-and-shoot IMRT. *Phys Med Biol* 2004;49:N175–N179.
33. Seco J, Sharp GC, Turcotte J, *et al.* Effects of organ motion on IMRT treatments with segments of few monitor units. *Med Phys* 2007;34:923–934.
34. Noel CE, Santanam L, Olsen JR, *et al.* An automated method for adaptive radiation therapy for prostate cancer patients using continuous fiducial-based tracking. *Phys Med Biol* 2010;55:65–82.
35. Plathow C, Schoebinger M, Fink C, *et al.* Quantification of lung tumor volume and rotation at 3D dynamic parallel MR imaging with view sharing: Preliminary results. *Radiology* 2006;240:537–545.